Supporting Information

Dual-Emission Fluorescent Sensor Based on AIE Organic Nanoparticles and Au Nanoclusters for the Detection of Mercury and Melamine

Caixia Niu,[a] Qiuling Liu,[a] Zhehai Shang,[a] Liu Zhao,[a] and Jin Ouyang,[a]*

[a] Key Laboratory of Theoretical and Computational Photochemistry, Ministry of Education, College of Chemistry, Beijing Normal University, Beijing 100875, China. Fax: 861062799838; Tel: 861058805373; E-mail: jinoyang@bnu.edu.cn

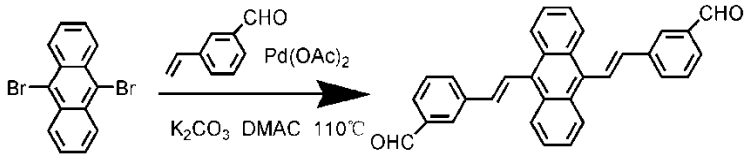

Scheme S1. Synthesis routes of 9,10-bis(3-formylstyryl)anthracene (BFSA).

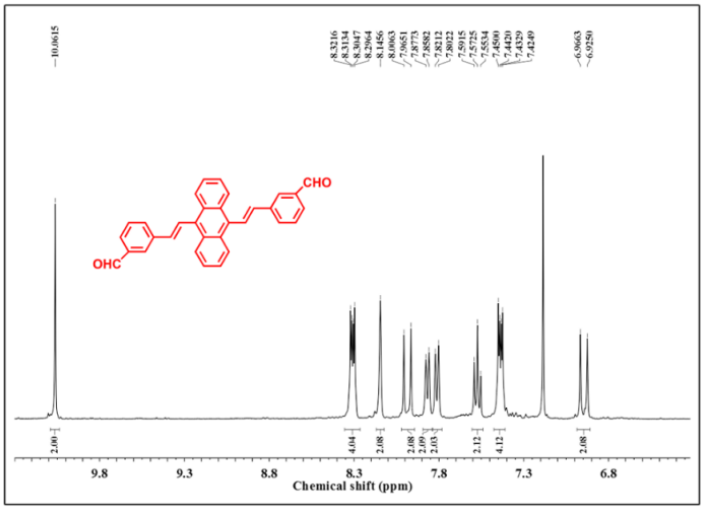

Figure S1. ^{1}H NMR spectrum ($CDCl_3$, 400 MHz) of BFSA.

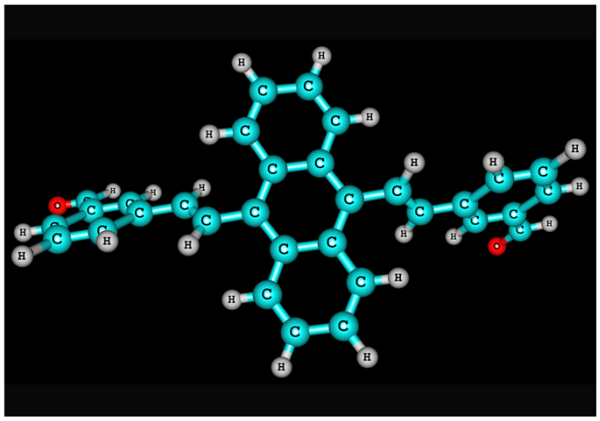

Figure S2. Optimized molecular structure of BFSA.

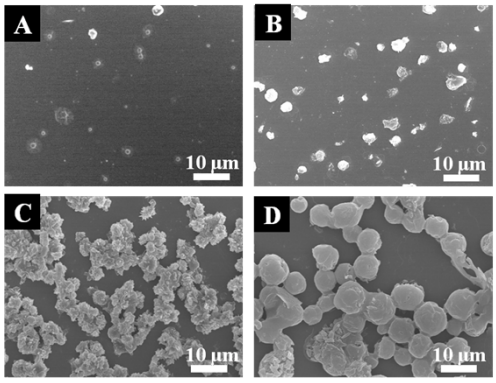

Figure S3. Scanning electron microscope (SEM) micrographs of BFSA generated by evaporating suspensions of THF/water mixtures with f_w =60%, f_w =70%, f_w =80%, f_w =90%, respectively.

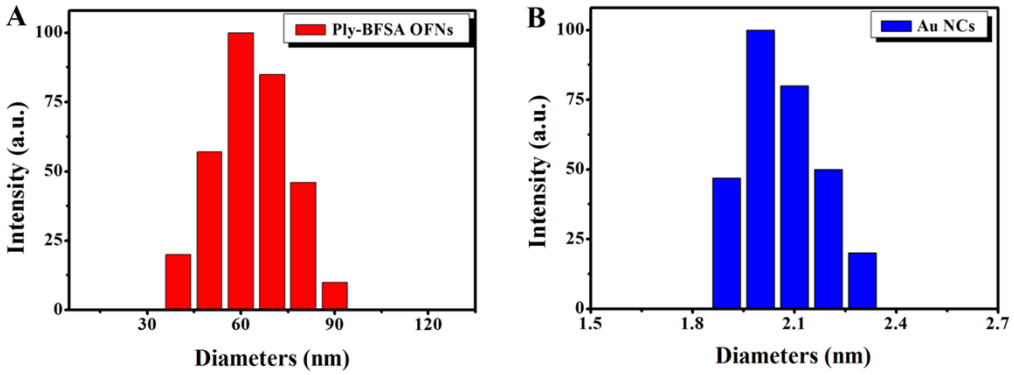

Figure S4. DLS results of A) Ply-BFSA OFNs and B) Au NCs.

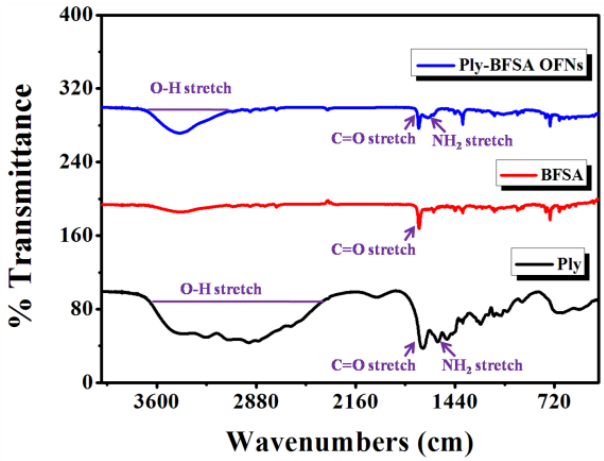

Figure S5. FT-IR spectra of Ply (blank line), BFSA (red line) and Ply-BFSA OFNs (blue line).

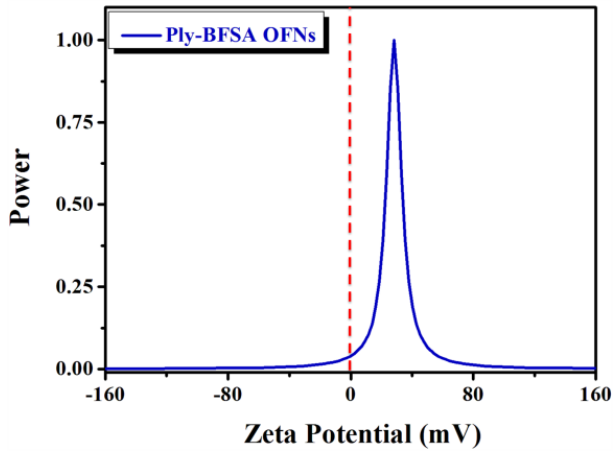

Figure S6. Zeta potential of Ply-BFSA OFNs.

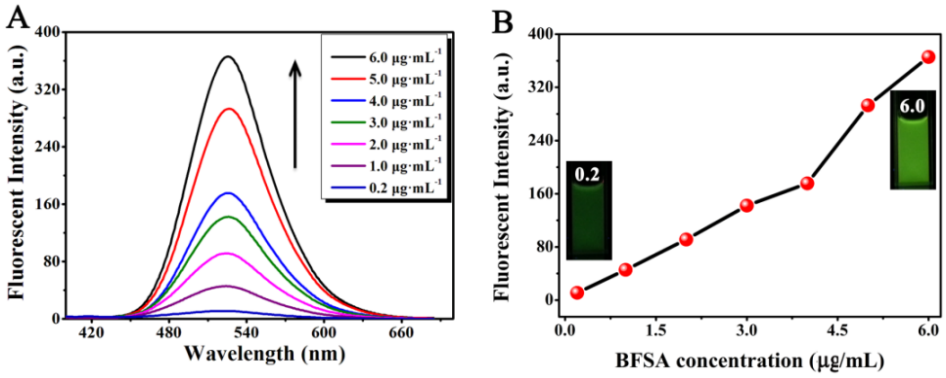

Figure S7. A) Fluorescence (FL) spectra and B) corresponding FL intensity of Ply-BFSA OFNs in water with different water concentrations exited at 360 nm. Inset: Fluorescent pictures of Ply-BFSA OFNs in water with the concentrations of 0.2 and 6.0 μg·mL^{-1}.

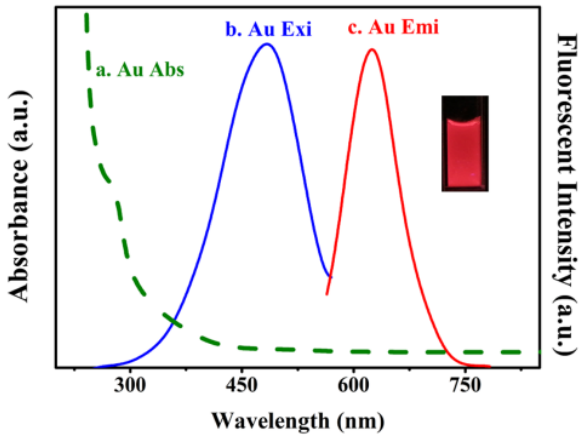

Figure S8. Absorption (dash green line), excitation (solid blue line), emission (solid red line) spectra, and fluorescent pictures (insert) of aqueous solution of Au NCs.

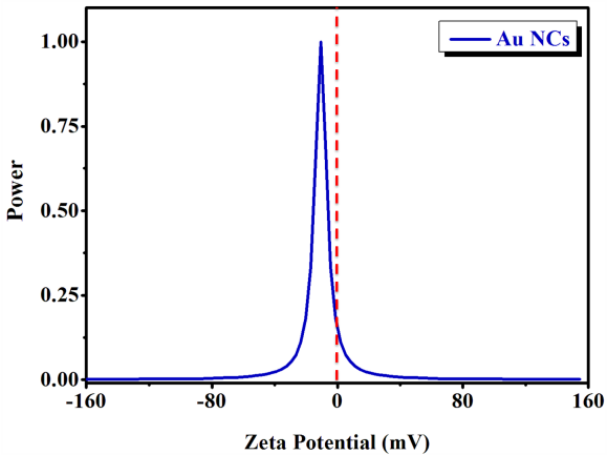

Figure S9. Zeta potential of Au NCs.

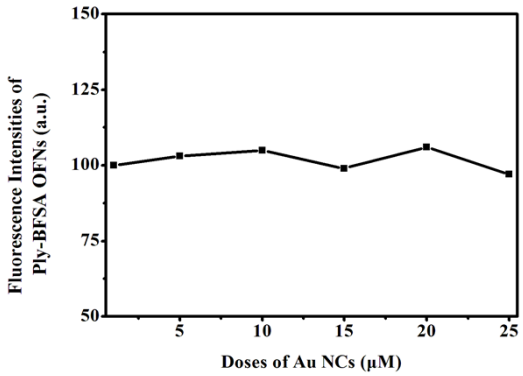

Figure S10. The fluorescence intensities of OFNs (1.6 μg·mL^{-1}) with different doses of Au NCs.

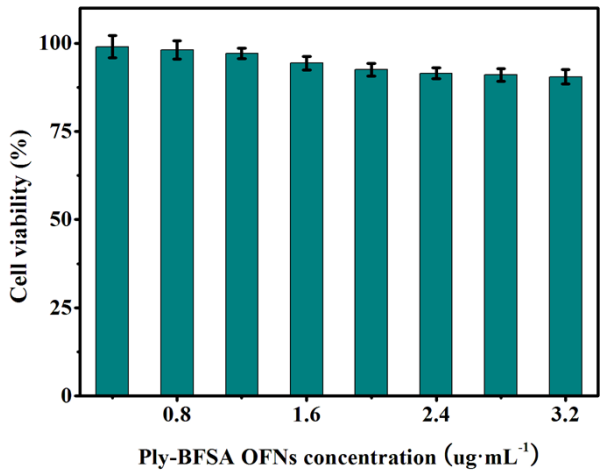

Figure S11. MTT assay of HeLa cells treated with different concentrations of Ply-BFSA OFNs for 24 h.

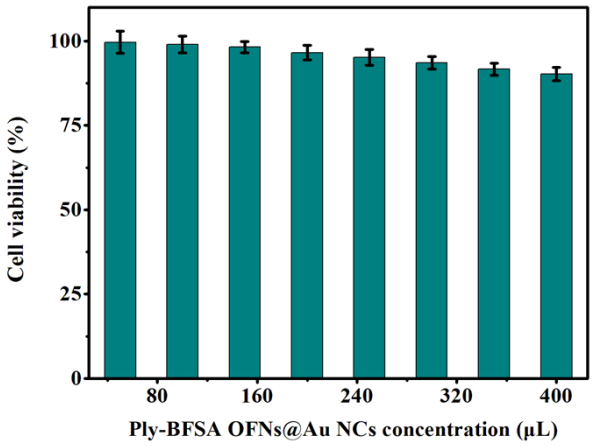

Figure S12. MTT assay of HeLa cells treated with different concentrations of Ply-BFSA OFNs@Au NCs for 24 h.

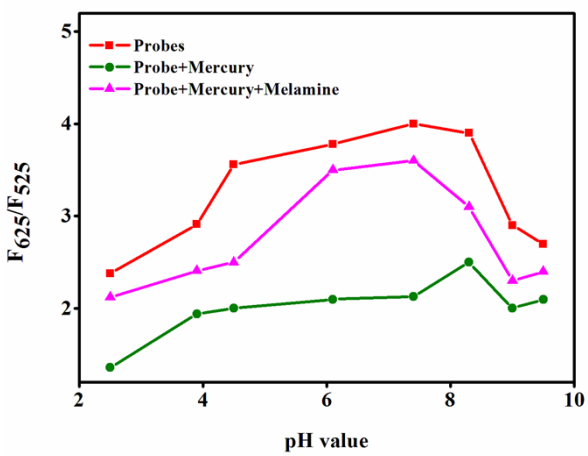

Figure S13. The fluorescence intensity ratios F_{625}/F_{525} of dual-emission nanoprobes (red line), nanoprobe with Hg^{2+} (green line), and nanoprobe with Hg^{2+} and melamine (pink line).

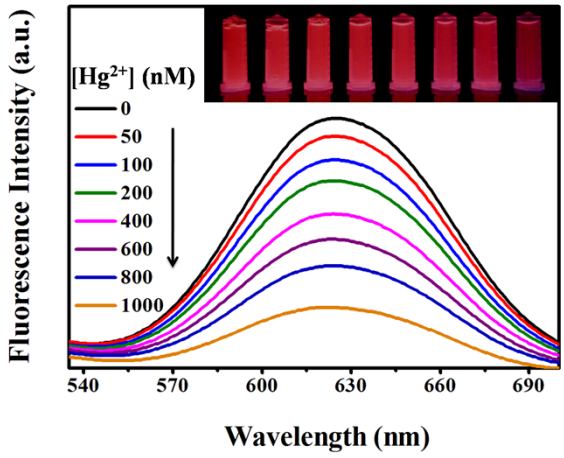

Figure S14. Fluorescence emission spectra of the Au NCs upon exposure to different concentrations of Hg^{2+}. The inset photos show the corresponding fluorescence colors under UV illumination, respectively.

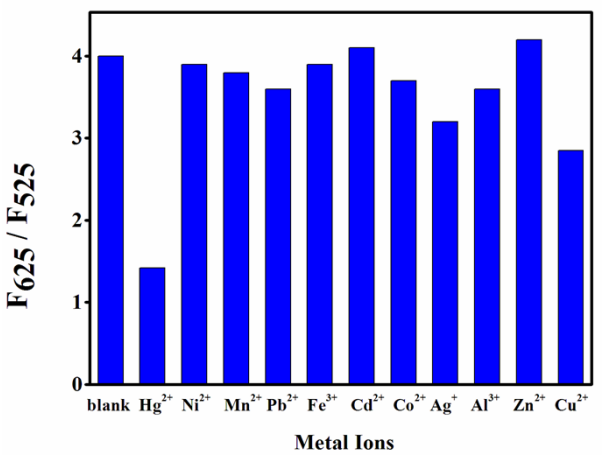

Figure S15. The fluorescence intensity ratios F_{625}/F_{525} of dual-emission nanoprobes with various metal ions (Hg^{2+}, Ni^{2+}, Mn^{2+}, Pb^{2+}, Fe^{3+}, Cd^{2+}, Co^{2+}, Ag^{+}, Al^{3+}, Zn^{2+}, and Cu^{2+} at 800 nM) in PBS (10 mM, pH=7.4)

Equation for the calculate binding constant:

$$\log\frac{F_0 - F}{F} = \log Ka + n\log[Q] \quad \textbf{(1)}$$

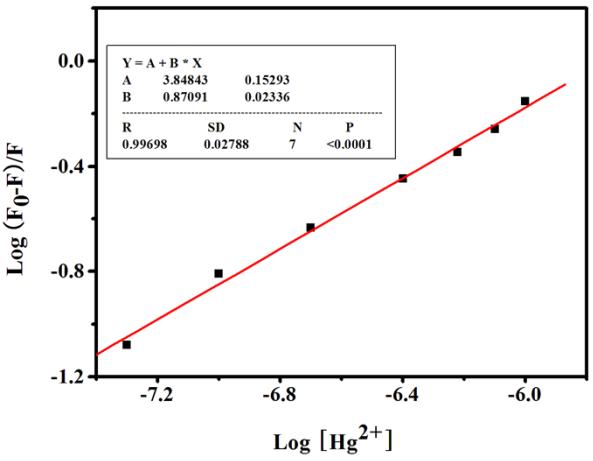

Figure S16. The double-log plots of Hg^{2+} quenching effects on Au NCs.

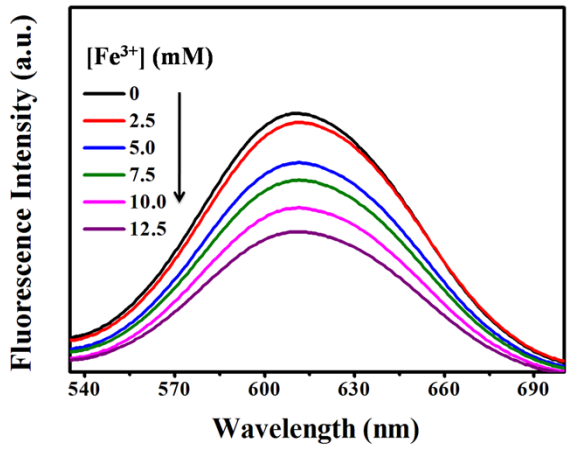

Figure S17. Fluorescence emission spectra of the Au NCs upon exposure to different concentrations of Fe^{3+}.

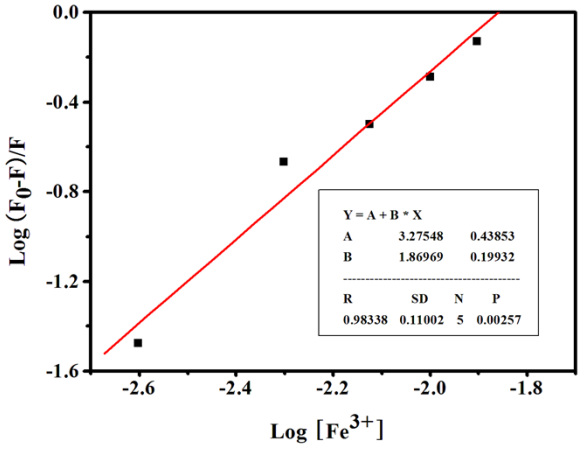

Figure S18. The double-log plots of Fe^{3+} quenching effects on Au NCs.

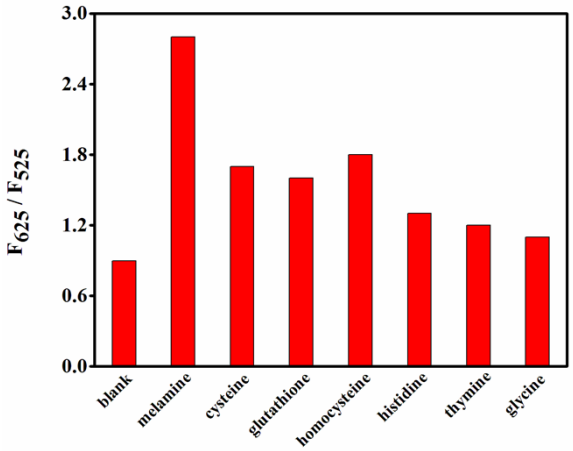

Figure S19. The fluorescence intensity ratios F_{625}/F_{525} of dual-emission nanoprobes with melamine, cysteine, glutathione, homocysteine, histidine, thymine and glycine at 20 μM in PBS (10 Mm, pH=7.4).

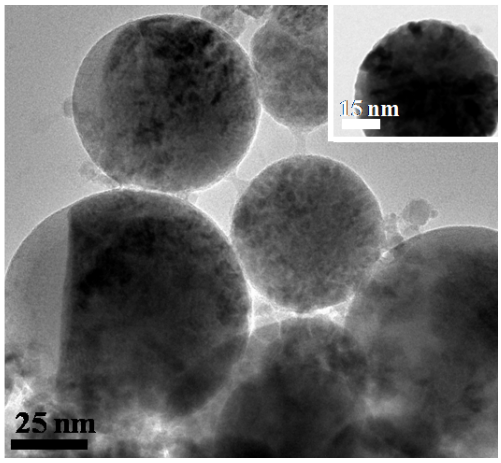

Figure S20. Ply-BFSAOFNs@Au NCs dispersed in 1% human serum (bar: 25 nm), insert picture shows the surface of Ply-BFSA OFNs@Au NCs (bar: 15 nm).

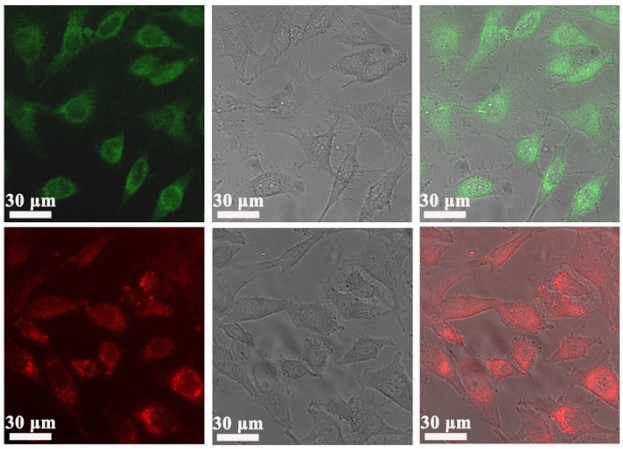

Figure S21. Fluorescence images of HeLa cells after incubation with Ply-BFSA OFNs for 4 h; Solvents are THF/water mixtures with f_w=99.5 %; Excitation wavelength is 405 nm. A) fluorescence images; B) bright-field images; C) merged images of the fluorescence images and bright-field images. Fluorescence images of HeLa cells after incubation with Ply-BFSA OFNs@Au NCs for 4 h; Solvents are THF/water mixtures with f_w=99.5 %; Excitation wavelength is 405 nm.D) Fluorescence images; E) bright-field images; F) merged images of the fluorescence images and bright-field images.

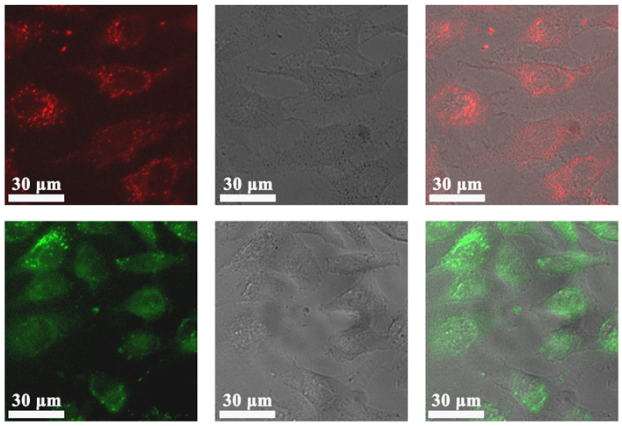

Figure S22. Fluorescence images of HeLa cells after incubation with Ply-BFSA OFNs@Au NCs for 4 h; Solvents are THF/water mixtures with f_w=99.5 %; Excitation wavelength is 405 nm. A) fluorescence images; B) bright-field images; C) merged images of the fluorescence images and bright-field images. Fluorescence images of HeLa cells after incubation with Hg^{2+} (400 nM) for 1 h and Ply-BFSA OFNs@Au NCs for 4 h; Solvents are THF/water mixtures with f_w=99.5 %; Excitation wavelength is 405 nm. D) Fluorescence images; E) bright-field images; F) merged images of the fluorescence images and bright-field images.

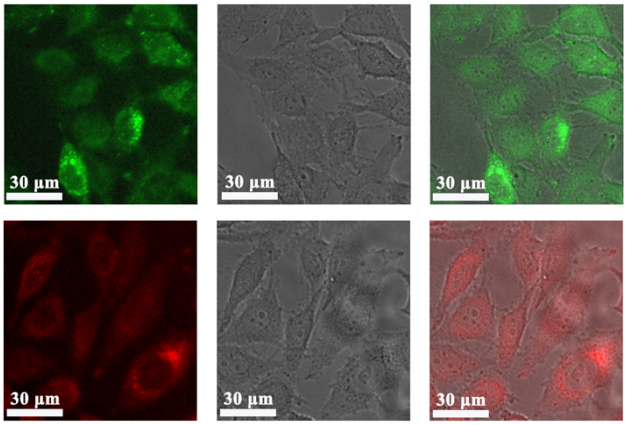

Figure S23. Fluorescence images of HeLa cells after incubation with Hg^{2+} (200 nM) for 1 h and Ply-BFSA OFNs@Au NCs for 4 h; Solvents are THF/water mixtures with f_w=99.5 %; Excitation wavelength is 405 nm. A) fluorescence images; B) bright-field images; C) merged images of the fluorescence images and bright-field images. Fluorescence images of HeLa cells after incubation with Hg^{2+} (200 nM) and

melamine (6 μM) for 1 h and Ply-BFSA OFNs@Au NCs for 4 h; Solvents are THF/water mixtures with f_w=99.5 %; Excitation wavelength is 405 nm. D) Fluorescence images; E) bright-field images; F) merged images of the fluorescence images and bright-field images.

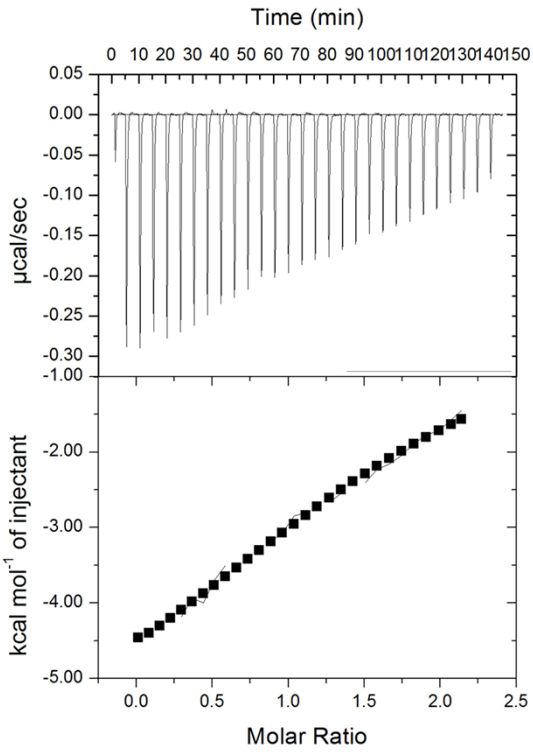

Figure S24. ITC profile for the binding of Hg^{2+} and melamine.

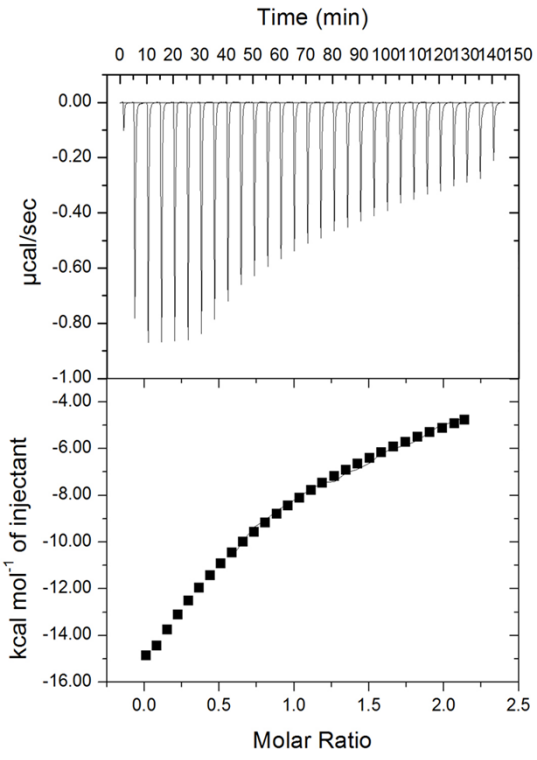

1

2 **Figure S25.** ITC profile for the binding of Hg^{2+} and GSH

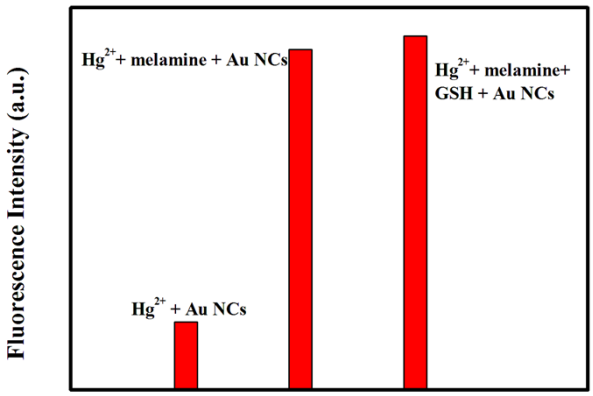

3

4 **Figure S26.** Fluorescence intensities of Hg^{2+} (200 nM) and Au NCs; Hg^{2+} (200 nM),
5 melamine (6 µM) and Au NCs; Hg^{2+} (200 nM), melamine (6 µM), GSH (10 mM) and
6 Au NCs.